Electronic Supplementary Material (ESI) for Soft Matter.

Supplementary Information

Shape Transitions in Network Model of Active Elastic Shells

Ajoy Maji[a], Kinjal Dasbiswas [b], Yitzhak Rabin[c]

[a]Faculty of Biomedical Engineering, Technion-Israel Institute of Technology, 32000 Haifa, Israel

[b] Department of Physics, University of California, Merced, Merced, CA 95343, USA

[c] Department of Physics and Institute of Nanotechnology and Advanced Materials, Bar-Ilan University, Ramat-Gan 5290002, Israel

Virtual triangulation of the network:

The 364 quadrilaterals are virtually triangulated by finding the center of mass of each of the quadrilateral and virtually connecting the center of mass to each of the vertices of that quadrilateral.

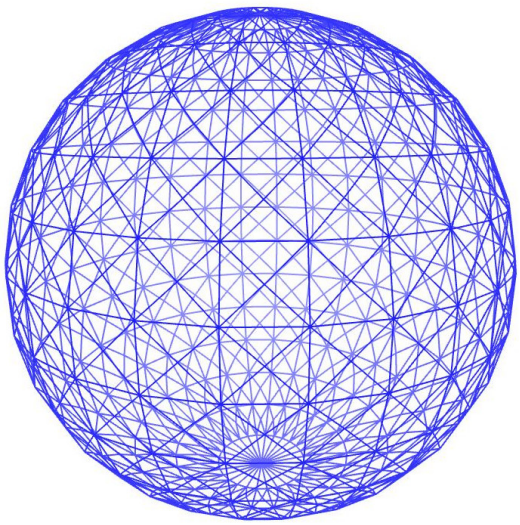

Fig. S 1: Snapshot of the virtually triangulated network

We introduce the hydrostatic force $\vec{F}_k^h$ on vertex k as the vector sum of the area of the triangles that meet at this vertex. $m = 28$ for the two poles, $m = 6$ for vertices that lie on the latitudinal circles next to the poles, and $m = 8$ for all other vertices.

$$\vec{F}_k^h = p \sum_{i=1}^{m} a_i \hat{n}_i \tag{1}$$

Where $\vec{a_i} = a_i \hat{n}_i$ is the area vector of the i^{th} triangle. The total area of the network is given by

$$\vec{A} = \sum_{i=1}^{1456+56} \vec{a}_i \tag{2}$$

Integration algorithm

$$\frac{d}{dt}(e^{\zeta t}\, \vec{v}_k) = e^{\zeta t} \vec{F}_k$$

Integrating both sides of this equation,

$$\int_{-\Delta/2}^{t} dt' \frac{d}{dt'}(e^{\zeta t'}\ \vec{v}_k) = \int_{-\Delta/2}^{t} dt'\ \vec{F}_k\ e^{\zeta t'} \tag{3}$$

where Δ is the MD time step which we take to be much shorter than the viscous damping time (mass/(friction coefficient)).

Solving equation 3, we get the following expressions for updating the velocity and position of vertex K:

$$\vec{v}_k((n+\frac{1}{2})\Delta) = \vec{v}_k((n-\frac{1}{2})\Delta)e^{-\zeta\Delta} + e^{-\zeta\frac{\Delta}{2}}\ \Delta\ \vec{F}_k(\vec{r}_k(n\Delta)) \tag{4}$$

$$\vec{v}_k(t) = \vec{v}_k(-\frac{\Delta}{2})e^{-\zeta(t+\Delta/2)} + e^{-\zeta\ t}\int_{-\Delta/2}^{t} dt'\vec{F}_k(t')e^{\zeta t'}$$

$$\implies \vec{v}_k(\tfrac{\Delta}{2}) = \vec{v}_k(-\tfrac{\Delta}{2})e^{-\zeta\Delta} + \Delta\vec{F}_k(\vec{r}_k(t=0))e^{-\zeta\frac{\Delta}{2}}$$

In general,

$$\vec{v}_k((n+\frac{1}{2})\Delta) = \vec{v}_k((n-\frac{1}{2})\Delta)e^{-\zeta\Delta} + e^{-\zeta\frac{\Delta}{2}}\ \Delta\ \vec{F}_k(\vec{r}_k(n\Delta)) \tag{5}$$

where n is the number of MD time steps.
The equation for the position can be written as,

$$\vec{r}_k(t) = \vec{r}_k(0) + \int_0^t \vec{v}_k(t')dt'$$

At $t = \Delta$,

$$\vec{r}_k(\Delta) = \vec{r}_k(0) + \Delta\ \vec{v}_k(\Delta/2)$$

In other words,

$$\vec{r}_k((n+1)\Delta) = \vec{r}_k(n\Delta) + \Delta\ \vec{v}_k\ ((n+\frac{1}{2})\Delta) \tag{6}$$

We are using equation 5 and 6 for updating velocities and positions of the vertices

Representation of the angles between the tangent of the neighboring springs:

θ_i is the angle between the tangents of i^{th} and $i-1^{th}$ spring. θ_{i+1} is the angle between the tangents of i^{th} and $i+1^{th}$ spring.

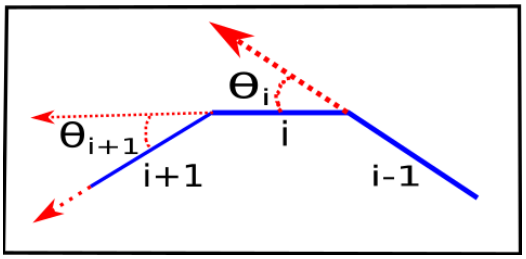

Fig. S 2: Representation of the angles between the tangents of the neighboring springs

Steady state configuration of the network with $p_0 = 0.1$

The network takes an oblate spheroid shape in steady state with $p_0 = 0.1$, in the absence of active excitations. The distance between two poles (D) and the diameter of the equatorial plane (2R) are marked. The ratio of D/2R represents the aspect ratio of the shape.

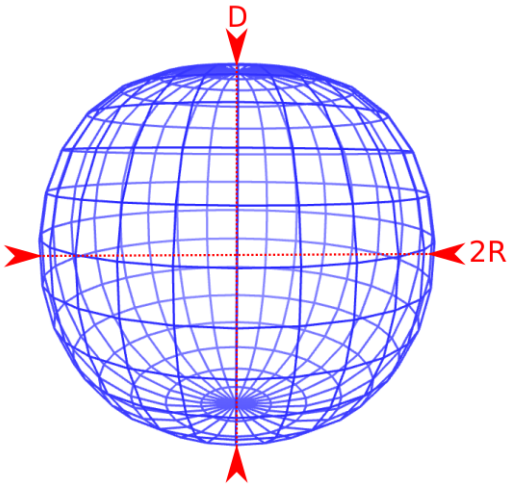

Fig. S 3: Steady state configuration of the network with $p_0 = 0.1$ before active excitations are switched on.

Model 2. Curvature-dependent relaxation of activation: pressure-induced discontinuous transition from prolate to oblate ellipsoids

We begin again from the spheroidal configuration of the network at pressure $p_0 = 0.1$ (Figure S3). Just as in model 1 activity is switched on at $t = 500$ and the elastic constants of all springs whose instantaneous curvature is lower than $\chi_c = 0.05$ are reduced from 1 to 0.05. Simultaneously, the hydrostatic pressure is dropped from 0.1 to some lower value, p. If the curvature of a spring goes above χ_c in the course of dynamics, the spring constant of that spring returns to its equilibrium value $K_{eq} = 1$.

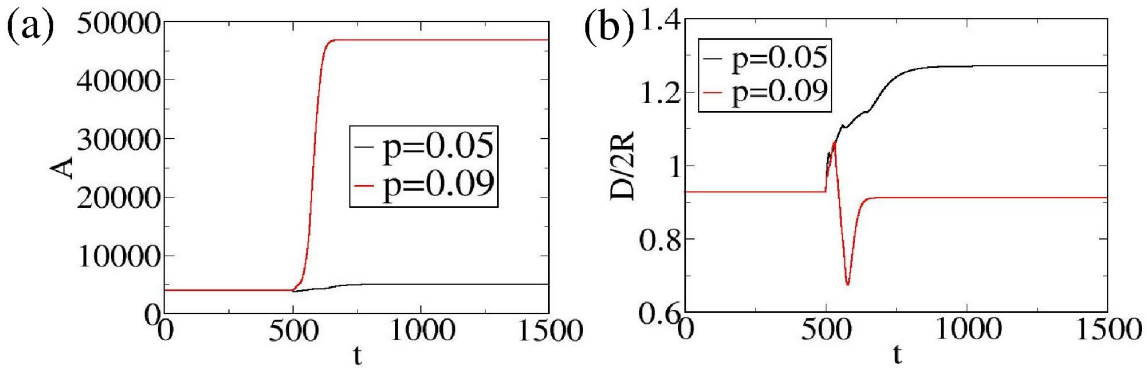

Fig. S 4: Model 2: (a) Area A and (b) aspect ratio $D/2R$ as a function of time for $p = 0.05$ (black) and $p = 0.09$ (red).

The area and the aspect ratio of model 2 are plotted as a function of time in Figures S4 (a) and (b) respectively, for $p = 0.05$ and $p = 0.09$. Slight differences between models 1 and 2 are observed at lower pressure, $p = 0.05$: in particular, the introduction of curvature-dependent relaxation in model 2 leads to lower area and aspect ratio compared to model 1 (Figure 3).

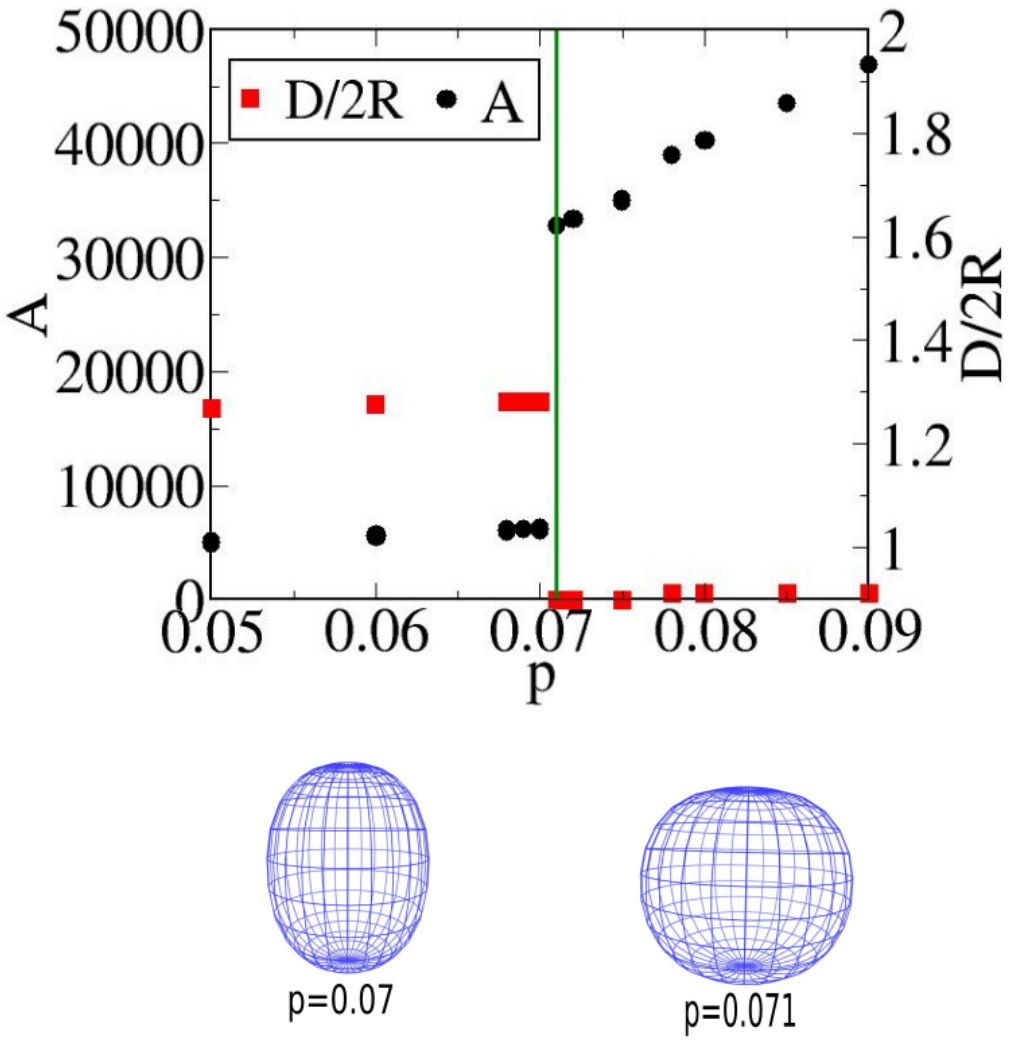

Fig. S 5: Model 2: area A and aspect ratio $D/2R$ are shown as a function of pressure. The location of the discontinuous transition is shown by the vertical broken green line. Snapshots of steady state configurations on both sides of the transition are presented in the lower panel (the snapshots are not to scale).

In Figure S5 we present the values of the area (black points) and the aspect ratio (red squares) in the final steady state of the actively excited network, for pressures in the range from 0.05 to 0.09, in the case of model 2. Similarly to model 1, a discontinuous transition from prolate to oblate ellipsoidal shape (accompanied by a jump of the total area of the network)

is observed between $p = 0.07$ and $p = 0.071$ (the dashed green vertical line in Figure S5). Snapshots of the steady state shapes of the system on both sides of the transition, at $p = 0.07$ and $p = 0.071$, are shown in the lower panel. Comparison of Figures 4 and S5 shows that the transition is shifted to slightly higher pressures and that the aspect ratios of the prolate ellipsoids for $p < p_c$ are lower in model 2 than in model 1.

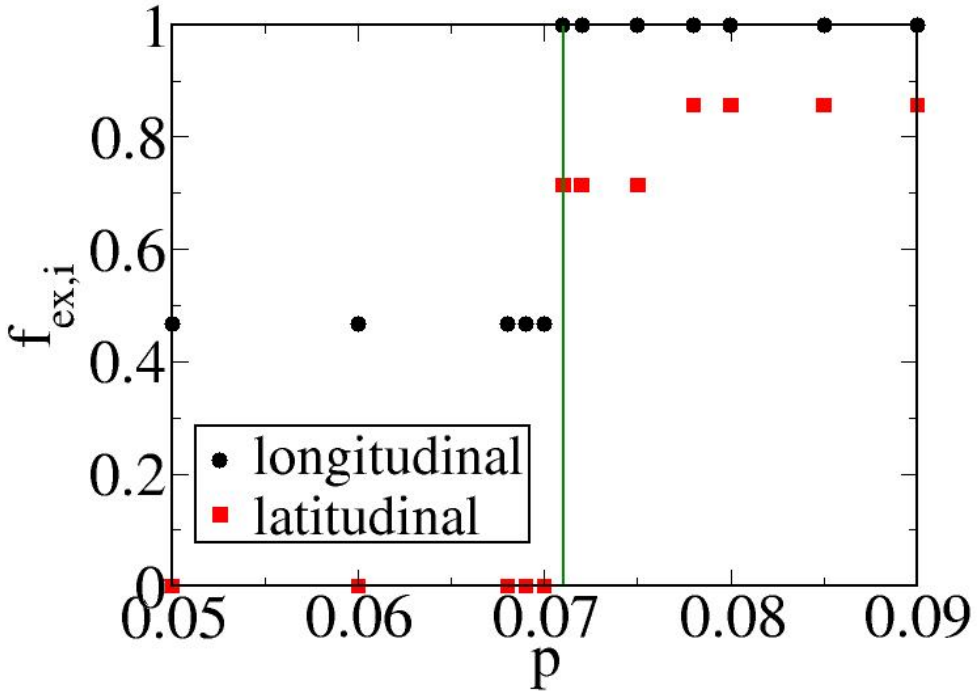

Fig. S 6: Model 2: Fractions of longitudinal and latitudinal activated springs in the excited steady state, as a function of pressure p.

In Figure S6 we present the fractions of activated longitudinal and latitudinal springs for different pressures in the range $0.05 - 0.09$. Comparison with Figure 6 shows that relaxation does not affect the size of the jump in the fraction of excited latitudinal springs but increases the discontinuity in the fraction of excited longitudinal springs across the transition.

Model 3: Curvature Distributions

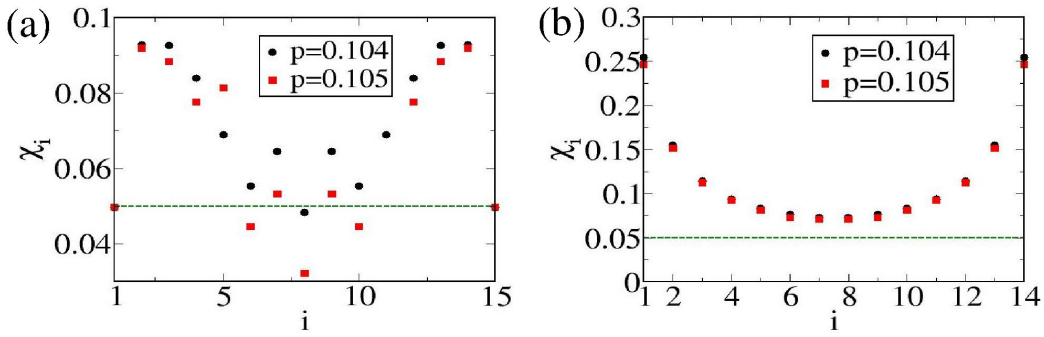

Fig. S 7: Model 3: Curvature distributions of (a) longitudinal and (b) latitudinal springs below and above p_{c1}, at $p = 0.104$ and $p = 0.105$, respectively.

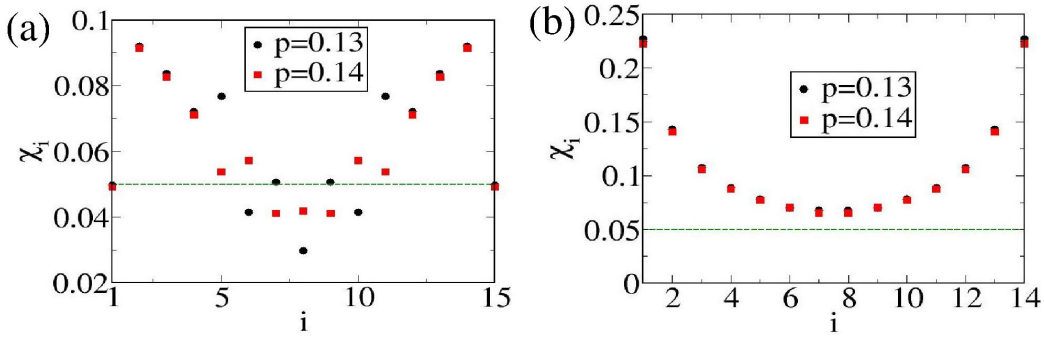

Fig. S 8: Model 3: Curvature distributions of (a) longitudinal and (b) latitudinal springs at $p = 0.13$ and $p = 0.14$.

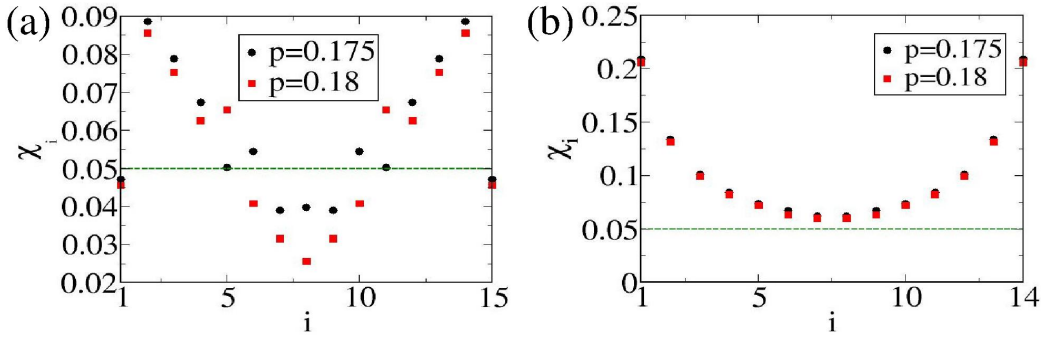

Fig. S 9: Model 3: Curvature distributions of (a) longitudinal and (b) latitudinal springs at $p = 0.175$ and $p = 0.18$.

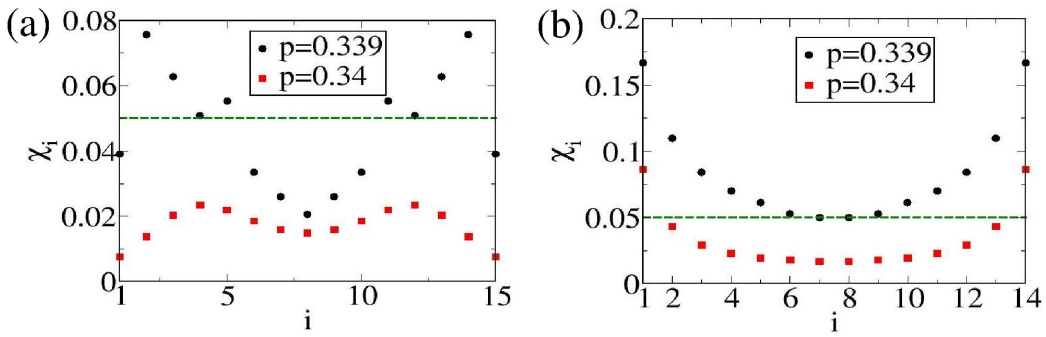

Fig. S 10: Model 3: Curvature distributions of (a) longitudinal and (b) latitudinal springs below and above p_{c2}, at $p = 0.339$ and $p = 0.34$, respectively.

Movies:

M1: Model 1: Time evolution of the network to steady state with $p = 0.09$. Initially longitudinal springs are excited, but as swelling proceeds, latitudinal springs also get excited which leads to a runaway radial expansion of the network normal to the polar axis.

M2: Model 1: Time evolution of the network to steady state with $p = 0.05$. Swelling of the network under this comparatively lower p value do not activate the latitudinal springs. The activation of the longitudinal springs leads to a prolate shape of the network.

M3: Model 1: The time evolution of the network to steady state for $p = 0.0653$, just before the transition to happen. Time evolution of the network at $p = 0.0653$ is very much similar to $p = 0.05$ (Movie M2) .

M4: Model 1: The time evolution of the network to steady state for $p = 0.0654$, just after the transition happens. Initially the activation of the longitudinal springs leads to a transient prolate shape of the network. But as the swelling progress, the latitudinal springs get activated and a dramatically swollen oblate spheroid results.

M5: Model 3: The time evolution of the network to steady state for $p = 0.02$. Since at t=0, the curvatures of most of the springs lie above χ_c, the activation of the springs leads to contraction of the network, which fur-

ther increases the curvature of the springs. The shrinking of the area becomes a runaway process which ultimately relaxes to oblate spheroid.

M6: Model 3: The time evolution of the network to steady state for $p = 0.2$. Contraction of most of the activated springs is opposed by the increment of pressure. The elongation of the longitudinal springs leads to a prolate spheroid shape of the network.

M7: Model 3: The time evolution of the network to steady state for $p = 0.4$. At this high pressure value, the latitudinal springs also get activated along with longitudinal springs. This leads to an oblate spheroid shape of the network.